ChemComm

Accepted Manuscript

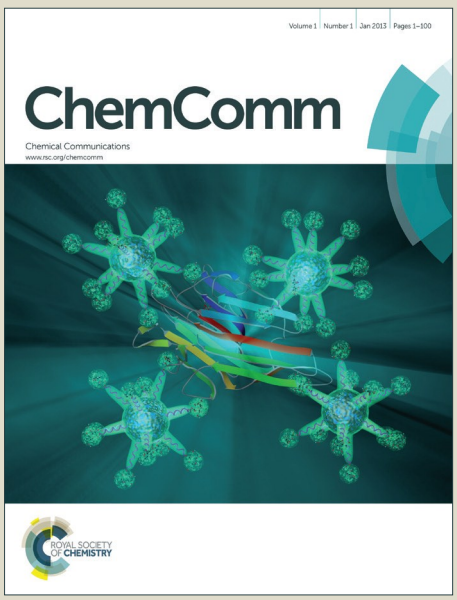

ROYAL SOCIETY OF CHEMISTRY

www.rsc.org/chemcomm

ChemComm

COMMUNICATION

Synthesis of self-reporting polymeric nanoparticles for *in situ* monitoring endocytic microenvironmental pH

Received 00th January 20xx,
Accepted 00th January 20xx

DOI: 10.1039/x0xx00000x

www.rsc.org/

Zeng-Ying Qiao, Chun-Yuan Hou, Wen-Jing Zhao, Di Zhang, Pei-Pei Yang, Lei Wang* and Hao Wang*

The bis(pyrene) conjugated pH-sensitive polymers (P-BP) were synthesized and self-assembled into nanoparticles through hydrophobic interactions. The Nile red (NR) loaded P-BP nanoparticles showed red emission due to the FRET effect. The nanoparticles entered cells by endocytosis, and the microenvironmental pH in the endocytosis process was *in situ* monitored by the simultaneous dual-wavelength fluorescence changes.

Nanomaterials have been developed intensively in the biological and medical fields due to their ability of improving diagnosis and treatment of diseases (termed nanomedicine).[1-4] Because of the nano-scaled size, nanomedicine with longer retention time and improved biodistribution can accumulate into tumor sites *via* enhanced permeability and retention (EPR) effect in the body. The precise spatiotemporal control of nanomedicine delivery in cellular level plays a vital role in targeted and specific imaging and therapy. Therefore, many efforts have been devoted to study the transportation of nanomedicine in cells, especially for the pathway of entrance into cells.[5-8] Most of nanomedicines are taken up by cells through endocytosis process, in which the endocytic vacuoles were transformed from endosomes to lysosomes with the pH decrease.[9] Hence, the pH values of endocytic organelles have important effect on the nanomedicine, such as the stability and controlled drug release from the nanocarriers in endocytic organelles, impacting on the imaging performance and therapeutic efficacy subsequently.[10-14]

A large amount of fluorescent probes such as organic dyes, fluorescent protein and inorganic compounds were developed for imaging the acidic microenvironment by the pH-dependent changes in wavelength and intensity of emission.[15-21] Recently, a pH probe with aggregation-induced emission properties realized full-range intracellular pH sensing.[22] In addition, the Förster resonance energy transfer (FRET) occurring through dipole-dipole interactions between excited donors (D) and acceptors (A) also have been applied for determination of pH.[23, 24] The pH values of endocytic organelles were determined by colocalization with pH sensor. As a result, the indirect method could not reflect the pH value in nanomedicine microenvironment accurately. It remains a challenge for *in situ* monitoring pH of endocytic organelles in endocytosis process.

Herein, we demonstrated a pH-sensitive nanoparticle with FRET effect to *in situ* monitor the microenvironmental pH around nanoparticles in endocytosis process. The bis(pyrene) (BP) was chosen as donors because it can form fluorescence *J*-type nanoaggregates through hydrophobic and π-π interactions in water, not aggregation-caused quenching.[25, 26] The BP was conjugated with hydrophilic poly(amino ester)s (as a pH-sensitive carrier, **P-BP**). The **P-BP** could self-assemble into nanoparticles through hydrophobic interactions at neutral pH with BP as the hydrophobic core and **P** as the hydrophilic shell. The FRET was observed by encapsulating Nile red (NR) into nanoparticles with red fluorescence emission (Scheme 1). As the pH decreased, the protonation of polymer chains induced the swelling of nanoparticles with enhanced BP fluorescence because the NR was released and its fluorescence was quenched due to the aggregation in water to eliminate the FRET effect. After targeted entering into cells by endocytosis,

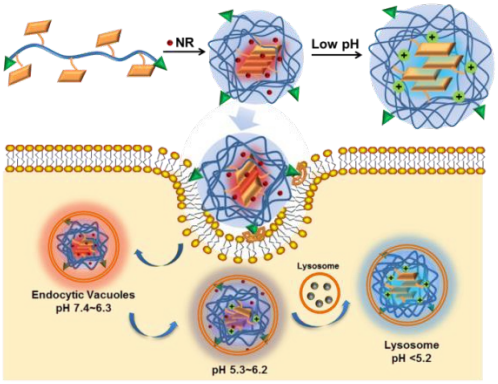

Scheme 1. Schematic illustration of ultra-sensitive NR-loaded **P-BP** nanoparticles for *in situ* monitoring microenvironmental pH in endocytosis process based on dual wavelength fluorescence changes.

CAS Key Laboratory for Biological Effects of Nanomaterials and Nanosafety, National Center for Nanoscience and Technology (NCNST), Beijing 100190, China. Email: wanghao@nanoctr.cn, wanglei@nanoctr.cn

† Electronic Supplementary Information (ESI) available: Experimental part (materials and methods), chemical characterization, nanoparticle properties, additional spectral and cellular data. See DOI: 10.1039/x0xx00000x

the nanoparticles could *in situ* monitor pH values according to the decrease of NR fluorescence and increase of BP fluorescence in living cells.

The copolymers poly(PEGDA-*co*-PA) (**P1-P3)** were first synthesized by Michael addition, obtaining polymers with different molecular weights by varying the molar ratios of two monomers (Scheme 2, Fig. S1a and Table S1).[27] **P3** with highest number of repeating units was utilized for further modification for linking more BP molecules. To obtain targeted polymers, the cyclic peptide c(RGDfC) was conjugated onto the ends of copolymer **P3**, and the almost complete disappearance of the peak at 5.9–6.5 ppm proved the efficient linkage of the targeted peptide (Fig. S1b).[28] **P-BP** was prepared by the click reaction between BP-N_3 (Fig. S2) and alkyne groups in RGD conjugated **P3** (**P**), the chemical structure of which was verified by ^{1}H NMR spectrum (Fig. 1a). The molar fraction of BP (~28%) was calculated by the area of peak 13 in BP molecules and peak 3 in polymer backbones. According to the polymerization degree of **P-BP** (DP ~17), the number of BP in a polymer chain was around 5. The BP molecules formed *J*-aggregate, which induced the self-assembly of polymer chains into nanoparticles with RGD targeted hydrophilic PEG chains as shells. The average hydrodynamic diameter of **P-BP** nanoparticles was ~41.7 nm measured by dynamic light scattering (DLS) at pH 7.4 (Fig. 1b), which was in accordance with the diameters of ~35±10 nm observed by transmission electron microscopy (TEM, Fig. 1c).

Due to the reversible protonation of tertiary amine groups in polymer chains, the copolymers are pH-sensitive, which was evaluated by a pH titration method (Fig. S3). After adding 0.1 M NaOH, a high buffer capacity of copolymers was observed in the range of pH 4.0–9.0 compared to NaCl solution, and the "proton sponge" effect of copolymers plays an important role in the pH-induced nanoparticles swelling.[29] The pH sensitive properties of **P-BP** nanoparticles were further investigated by DLS. At pH 7.4, the stable nanoparticles around 41.7 nm were measured. After addition of pH 5.0 buffer solution, the swollen

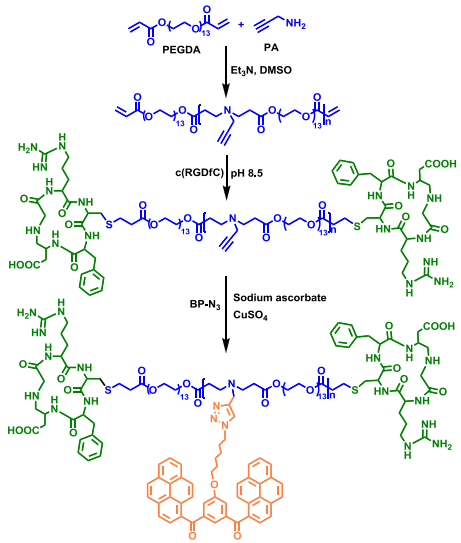

Scheme 2. The synthetic route of polymer **P-BP** with targeted RGD peptides and BP fluorescence groups.

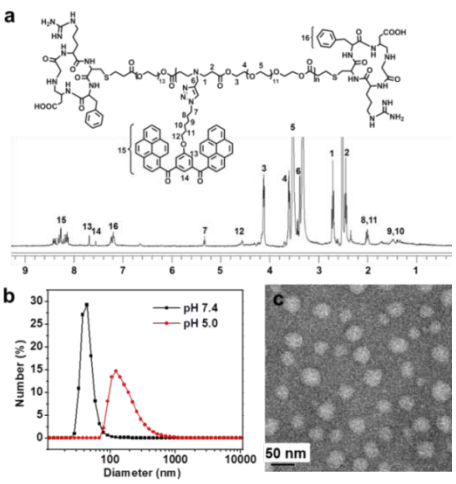

Fig. 1 (a) ^{1}H NMR spectrum of polymer **P-BP** in d^6-DMSO. (b) Number size distribution of **P-BP** nanoparticles (0.8 mg mL^{-1}) in PB solutions (10 mM, pH 7.4) and acetate b… (50 mM, pH 5.0) measured by DLS. (c) TEM images of **P-BP** in aqueous solutions at p… 7.4 (0.8 mg mL^{-1}).

nanoparticles with an average diameter of 138.2 nm w… observed, proving the ionization of polymer chains. Th… fluorescence spectra of **P-BP** nanoparticles at different pH… were further investigated to verify the pH-sensitiv… fluorescence changes (Fig. 2). The BP molecules in **P-B…** nanoparticles formed *J*-aggregates at pH 7.4 with emission peak at ~527 nm, which was in accordance with previou… reports.[25, 26] At pH 6.5, the appearance of peak at ~434 nm indicated that a part of the *J*-aggregates were destroyed. Th… acidic media induced the increased hydrophilicity of copolymer chains and the swelling of nanoparticles, separating th… conjugated BP in the copolymer chains from *J*-aggregates. As the pH was lowered to 5.5, only the peak at ~434 nm wa… examined, showing that the *J*-aggregates were disrupted totally. The separated BP could show the fluorescence with th… maxima at 434 nm inside the swollen nanoparticles. At mo… acidic condition of pH 5.0, the emission peak blue-shifted to ~418 nm, which was attributed to the further ionization of polymer chains and corresponding microeviromental changes.

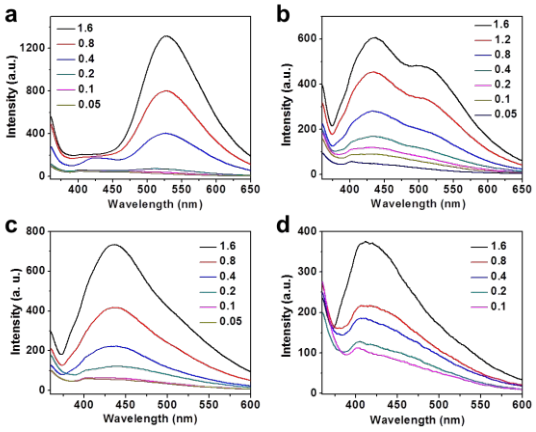

Fig. 2 Fluorescent emission spectra of the **P-BP** at (a) pH 7.4, (b) pH 6.5, (c) pH 5.5 and (d) pH 5.0 at different concentrations (mg mL^{-1}) in aqueous solutions. The excitati… wavelength: 350 nm.

inside the nanoparticles. In addition, as the concentration decreased to 0.1 mg mL^{-1}, the emission peak of BP monomer at ~403 nm was observed (Fig. 2). At higher concentration, even though the *J*-aggregates of BP were destroyed at acidic condition, the rotation of BP monomers was still restricted, causing the emission of BP ranging from 418 nm to 434 nm due to the microenviromental changes inside the nanoparticles. Therefore, the **P-BP** nanoparticles could be utilized as pH-sensitive fluorescence probe.

To extend the shift range of fluorescence at different pHs, NR was encapsulated into the **P-BP** nanoparticles for construction of FRET system. The *J*-aggregated BP was used as a donor and NR was selected as an acceptor, because the fluorescence emission spectrum of BP had a large overlap with the absorption spectrum of NR.[26] As the acceptor (NR) was added gradually, the fluorescence emission originated from donor (*J*-aggregated BP) was quenched gradually accompanied with increasing intensity of NR emission at ~628 nm (Fig. 3a). Upon the increase of NR up to > 6 μM in **P-BP** nanoparticle solution (200 μM), the fluorescence intensity at 635 nm became constant without further increase (Fig. S4). Compared with **P-BP** nanoparticles, the similar diameter (42.6 nm) at pH 7.4 and acid-induced swollen state (152.8 nm) of NR-loaded **P-BP** (**P-BP/NR**) nanoparticles were studied by DLS and TEM (Fig. S5). The diameters and fluorescence of **P-BP/NR** nanoparticles at pH 7.4 showed little change in 5 h, proving the good incubation stability of the nanoparticles (Fig. 3d and S6). The fluorescence spectra of **P-BP/NR** nanoparticles at various pHs were investigated (Fig. 3b). At acidic condition, the BP emission blue-shifted and the loaded NR was released from nanoparticles due to the ionization of polymer chains, resulting in the disappearance of FRET phenomenon. When the pH of **P-BP/NR** solution was lowered from 7.4 to 5.0, the emission intensity of NR at ~635 nm decreased gradually, and the emission intensity of BP at ~418 nm increased at the same time. The intensity ratios (R) of **P-BP/NR** at 418 nm to that at 635 nm (I_{418}/I_{635}) as a function of pH showed a standard pH calibration curve (Fig. 3c). Furthermore, as the pH decreased to 6.3/5.0, the NR emission intensity decreased rapidly in 2 min and then kept stable, which is due to the fast ionization of copolymer chains and subsequent NR release (Fig. 3d). Because of rapid fluorescence changes in 2 min, the fluorescence signal changes of **P-BP/NR** only related to pH rather than incubation time. The stability and the pH-responsiveness of **P-BP/NR** nanoparticles were further confirmed by measuring diameters and fluorescence spectra of **P-BP/NR** in various media (Fig. S7). There were no obvious changes in different conditions except pH decrease, verifying pH was the only effect on the swelling and fluorescence intensity of **P-BP/NR** nanoparticles. Therefore, the large fluorescence shift range of ~220 nm and ultrasensitive dual wavelength intensity changes make **P-BP/NR** nanoparticles as a promising tool to *in situ* monitor pH in endocytic organelles.

As we know, the RGD peptide can bind preferentially to the $\alpha_v\beta_3$ integrin which is over-expressed on some tumor cells, such as human primary glioblastoma (U87) cell.[30] To verify that the targeted **P-BP/NR** nanoparticles could enter into U87 cells

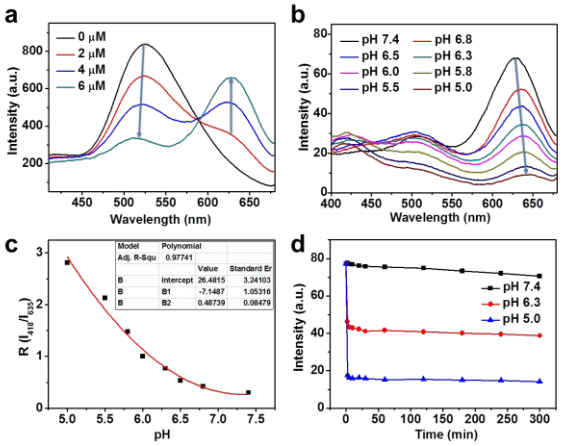

Fig. 3 (a) Fluorescence changes of NR-loaded **P-BP** nanoparticles (**P-BP/NR**) in emissi intensity at 524 nm and 628 nm upon gradual addition of NR (0, 2, 4 and 6 μM) in PB solutions (0.8 mg mL^{-1}, 10 mM, pH 7.4). (b) Fluorescence spectra changes of **P-BP/** solutions (0.08 mg mL^{-1}) with different pHs (7.4, 7.0, 6.8, 6.5, 6.0, 5.5 and 5.0). (c) The fluorescence intensity ratios (R) of **P-BP/NR** at 418 nm to that at 635 nm at variou values. (d) Incubation time-dependent change in the fluorescence intensity of **P-BP/NR** nanoparticles at different pHs. Concentration: 0.08 mg mL^{-1} for nanoparticles, 20 μM for BP. Temperature: 37 °C.

by receptor mediated endocytosis, lysosome colocalizatio with nanoparticles was investigated by confocal laser scanning microscopy (CLSM, Fig. 4). At the excitation wavelength of nm, the fluorescence emission of BP and NR could be observe in blue and red channel, respectively. The lysosomes of cel were stained with LysoTracker Green DND-26 which showed no fluorescence signal at the 405 nm excitation (Fig. S8). Afte incubation with cells for 40 min, the **P-BP/NR** nanoparticles were taken up by endocytosis, proved by the colocalization nanoparticles (blue and red signal) and lysosomes (green signal). By increasing the incubation time, the fluorescenc intensity of BP increased and the signal of NR decreased simultaneously, which could be attributed to the grad acidification of endocytic organelles in the transport process. At 120 min, the colocalization of BP and lysosome confirmed **P-BP/NR** could monitor microenvironmental pH in endocytosi process accurately in this time scale.

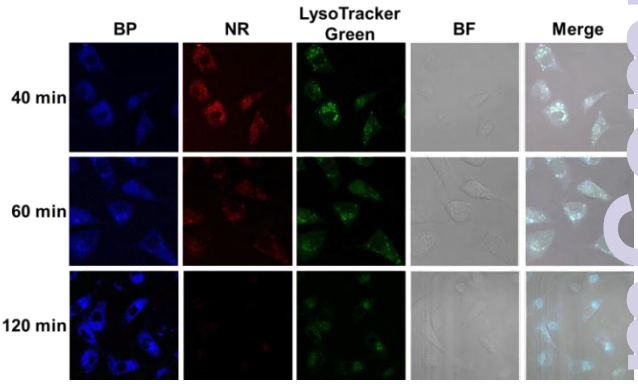

Fig. 4 CLSM microscopy of living U87 cells that were incubated with **P-BP/NR** for 40 m 60 min and 120 min, respectively. BF: bright field. Concentration: 0.08 mg mL^{-1} f nanoparticles, 20 μM for BP. Lysosomes were labeled with LysoTracker Green DND-26 for 30 min before imaging. Temperature: 37 °C. Excitation wavelength: 405 n Emission wavelengths: 410-430 nm (blue channel) and 625-645 nm (red channel).

After verifying the colocalization of **P-BP/NR** nanoparticles and endocytic organelles, the fluorescence signals in living U87 cells incubated with **P-BP/NR** were observed by CLSM *in situ* (Fig. 5). Through the efficient targeting of RGD, the nanoparticles were taken up by cells in 10 min with intense NR fluorescence and no BP emission, indicating that the pH of endocytic vacuoles were still neutral. At 20 min, the NR signal intensity decreased and BP signal appeared, and the intensity ratio of BP to that of NR (R) was 0.65, which showed the microenvironment became weakly acidic. As the time prolonged to 60 min, the pH was further decreased, since the R value became 1.55, which may imply the nanoparticles were located in endosome.[31] At 90 min, the R value was increased to 3.97, proving the endocytic organelles transformed into lysosomes (pH<5). In addition, the **P-BP/NR** nanoparticles showed no obvious cytotoxicity within the imaging concentration range (Fig. S9). Therefore, the pH of endocytic organelles could be *in situ* monitored by **P-BP/NR** nanoparticles in living cells.

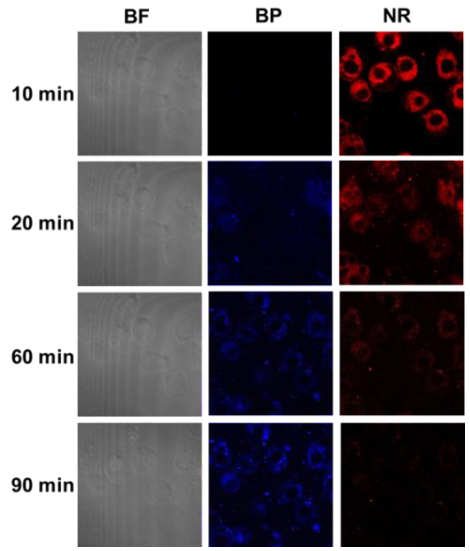

Fig. 5 *In situ* CLSM observation of living U87 cells that were incubated with **P-BP/NR** for 10 min, 20 min, 60 min and 90 min, respectively. Concentration: 0.08 mg mL^{-1} for nanoparticles, 20 μM for BP. Temperature: 37 ^{o}C. Excitation wavelength: 405 nm; Emission wavelengths: 410-430 nm (blue channel) and 625-645 nm (red channel).

In conclusion, we developed a BP conjugated polymer with pH ultrasensitive properties. The construction of FRET system by loading NR in **P-BP** nanoparticles realized the pH-induced dual-wavelength fluorescence changes. The **P-BP/NR** nanoparticles could be applied as potential pH sensor for *in situ* imaging endocytic organelles in living cells.

This work was supported by the National Natural Science Foundation of China (21304023, 21374026, 51473188 and 51303036), National Basic Research Program of China (973 Program, 2013CB932701) and the 100-Talent Program of the Chinese Academy of Sciences.

Notes and references

1. A. Wicki, D. Witzigmann, V. Balasubramanian and J. Huwyl, *J. Control. Release*, 2015, **200**, 138-157.
2. M. S. Shim and Y. J. Kwon, *Adv. Drug Del. Rev.*, 2012, **64**, 1046-1058.
3. V. Biju, *Chem. Soc. Rev.*, 2014, **43**, 744-764.
4. H. Ji, Y. Guan, L. Wu, J. Ren, D. Miyoshi, N. Sugimoto and X. Qu, *Chem. Commun.*, 2015, **51**, 1479-1482.
5. L. M. Bareford and P. W. Swaan, *Adv. Drug Del. Rev.*, 2007, **59**, 748-758.
6. A. C. Anselmo and S. Mitragotri, *J. Control. Release*, 2014, **190**, 531-541.
7. G. Sahay, D. Y. Alakhova and A. V. Kabanov, *J. Control. Release*, 2010, **145**, 182-195.
8. T.-G. Iversen, T. Skotland and K. Sandvig, *Nano Today*, 2011, **6**, 176-185.
9. J. R. Casey, S. Grinstein and J. Orlowski, *Nat. Rev. Mol. Cell Biol.*, 2010, **11**, 50-61.
10. Z.-Y. Qiao, R. Ji, X.-N. Huang, F.-S. Du, R. Zhang, D.-H. Liang and Z.-C. Li, *Biomacromolecules*, 2013, **14**, 1555-1563.
11. Z.-Y. Qiao, R. Zhang, F. S. Du, D. H. Liang and Z. C. Li, *J. Control. Release*, 2011, **152**, 57-66.
12. Z.-Y. Qiao, S.-L. Qiao, G. Fan, Y.-S. Fan, Y. Chen and H. Wang, *Polym. Chem.*, 2014, **5**, 844-853.
13. A. W. Jackson and D. A. Fulton, *Chem. Commun.*, 2011, **47**, 6807-6809.
14. A. Sanchez-Sanchez, D. A. Fulton and J. A. Pomposo, *Chem. Commun.*, 2014, **50**, 1871-1874.
15. W. Shi, X. Li and H. Ma, *Angew. Chem. Int. Ed.*, 2012, **51**, 6432-6435.
16. L. Cao, X. Li, S. Wang, S. Li, Y. Li and G. Yang, *Chem. Commun.*, 2014, **50**, 8787-8790.
17. Y.-N. Chen, P.-C. Chen, C.-W. Wang, Y.-S. Lin, C.-M. Ou, L.-C. Ho and H.-T. Chang, *Chem. Commun.*, 2014, **50**, 8571-8574.
18. T. Berbasova, M. Nosrati, C. Vasileiou, W. Wang, K. Sing, S. Lee, I. Yapici, J. H. Geiger and B. Borhan, *J. Am. Chem. Soc.*, 2013, **135**, 16111-16119.
19. M. Tantama, Y. P. Hung and G. Yellen, *J. Am. Chem. Soc.*, 2011, **133**, 10034-10037.
20. L. Wang, X. Zhu, C. Xie, N. Ding, X. Weng, W. Lu, X. Wei and C. Li, *Chem. Commun.*, 2012, **48**, 11677-11679.
21. H. Zhu, L. Gao, X. Jiang, R. Liu, Y. Wei, Y. Wang, Y. Zhao, Z. Chai and X. Gao, *Chem. Commun.*, 2014, **50**, 3695-3698.
22. S. Chen, Y. Hong, Y. Liu, J. Liu, C. W. T. Leung, M. Li, R. T. K. Kwok, E. Zhao, J. W. Y. Lam, Y. Yu and B. Z. Tang, *J. Am. Chem. Soc.*, 2013, **135**, 4926-4929.
23. R. J. Meier, J. M. B. Simburger, T. Soukka and M. Schaferling, *Chem. Commun.*, 2015, **51**, 6145-6148.
24. J.-C. Yu, Y.-L. Chen, Y.-Q. Zhang, X.-K. Yao, C.-G. Qian, J. Huang, S. Zhu, X.-Q. Jiang, Q.-D. Shen and Z. Gu, *Chem. Commun.*, 2014, **50**, 4699-4702.
25. L. Wang, W. Li, J. Lu, Y.-X. Zhao, G. Fan, J.-P. Zhang and H. Wang, *J. Phys. Chem. C*, 2013, **117**, 26811-26820.
26. P.-P. Yang, Y. Yang, Y.-J. Gao, Y. Wang, J.-C. Zhang, Y.-X. Lin, T. Dai, J. Li, L. Wang and H. Wang, *Adv. Optical Mater.*, 2014, **3**, 646-651.
27. A. Akinc, D. G. Anderson, D. M. Lynn and R. Langer, *Bioconjugate Chem.*, 2003, **14**, 979-988.
28. Z.-Y. Qiao, C. Hou, D. Zhang, Y. Liu, Y.-X. Lin, H.-W. An, X.-L. Li and H. Wang, *J. Mater. Chem. B*, 2015, **3**, 2943--2953.
29. J. J. Green, R. Langer and D. G. Anderson, *Acc. Chem. Res.*, 2008, **41**, 749-759.
30. F. Danhier, A. Le Breton and V. Preat, *Mol. Pharm.*, 2012, **9**, 2961-2973.
31. S. Modi, M. G. Swetha, D. Goswami, G. D. Gupta, S. Mayor and Y. Krishnan, *Nat. Nanotechnol.*, 2009, **4**, 325-330.